Tissue Localization of Stable and Radioactive Nuclides by Secondary-Ion Microscopy

Pierre Galle

Faculté de Médecine, Créteil, France

Images of the distribution of a given nuclide in a section of biological tissue can be obtained at the microscopic level by "secondary-ion mass analysis." In this method, the images are formed by an ion-emission microscope wherein the specimen's atoms are progressively sputtered from the surface and the ions are selectively visualized by mass spectrometry according to their mass-to-charge ratios. Such images are obtained at the cost of the destruction of the specimen, which is progressively eroded at the rate of 1–10 atomic layers per second.

The spatial resolution is better than 1 μm for an imaged area 250 μm in diameter and a section thickness of 1–2000 nm; thus, the analytical images are element distributions representative of 3–6000 atomic layers. Distributional images can be obtained for many nuclides, whether stable or radioactive, natural or artificially administered.

J Nucl Med 23: 52–57, 1982

Since 1945, a number of microanalytical methods have been proposed for the chemical analysis of microscopic volumes (1 cubic micron or less) in a solid sample. Among these methods, analytical ion microscopy, proposed by Castaing and Slodzian in 1960 (*1,2*) may be applied successfully to the study of biological specimens such as tissue sections (*3–5*). This method has two important characteristics: (a) its ability for a local isotopic analysis, and (b) is very high sensitivity, which allows the detection of elements at very low concentration. These characteristics permit the study of the tissue distribution of a given nuclide at the cellular level. The principles of the method, instrument specifications, and its limitations are presented here, along with some applications in the fields of cellular biology, nuclear medicine, and human pathology.

PRINCIPLES

An ion beam (primary ions) of seyeral keV energy is focused as a stable probe onto the surface of a tissue section. As a result of this ion bombardment, the atoms of the upper atomic layers of the specimen are sputtered (Fig. 1), and some come off in an ionized form (secondary ions). These secondary ions, characteristic of the composition of the surface of the specimen, are accelerated, focused as an ion beam, filtered by mass spectrometry, and imaged by an ionic optical system.

Most of these secondary ions are emitted from the first two or three atomic layers of the surface, although the primary ion beam produces perturbations to a depth of approximately 10 nm. As a result of the sputtering process, the surface of the specimen is progressively eroded, and the analysis is performed at the cost of the destruction of the volume analyzed.

INSTRUMENTATION

The analytical ion microscope* (Fig. 2) consists of four principal parts: an ion gun, which produces the bombarding primary ions, an electrostatic lens to accelerate and focus the secondary ions emitted from the specimen, a magnetic prism for the selection of ions, and a detection-display system.

Received Apr. 8, 1981; revision accepted Aug. 4, 1981.

For reprints contact: P. Galle, Département de Biophysique, Faculté de Médecine, 8, rue du Général Sarrail, 94000 Créteil, France.

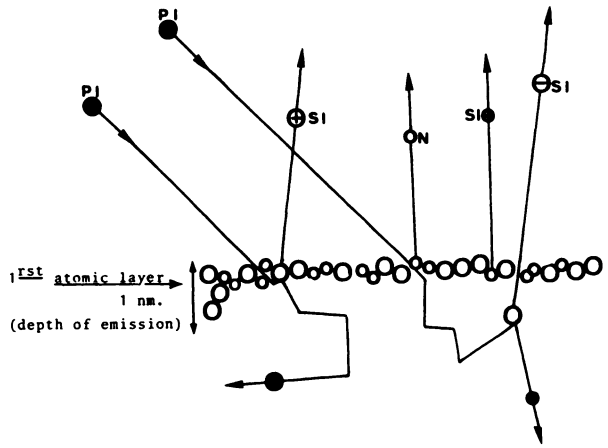

FIG. 1. Emission of positive and negative secondary ions (SI) and of neutral atoms (N) from first three atomic layers at surface of a solid bombarded by primary ions (PI).

Primary-Ion Source

This source produces a given variety of ions, generally O_2^+, Ar^+, or N^+. The primary ions are accelerated through a 12-kV potential and focused with a double-condenser electrostatic lens system onto the surface of the sample at approximately 45°. The bombarded area is typically 500 μm in diameter.

Electrostatic Optics

The secondary ions emitted from the surface of the specimen are accelerated by a potential of 4.5 kV, the polarity of which depends on the type of ion, positive or negative, that is being studied. An electrostatic lens focuses the secondary ions as a beam carrying a global image of all ions emitted from the specimen; this beam enters a magnetic prism.

Magnetic Prism

The role of the magnetic prism or spectrometer is to split the initial beam carrying the global image into a number of secondary beams, one for each mass/charge ratio in the secondary ions. A suitably placed aperture then makes it possible to select only one ionic component of the secondary beam.

The magnetic prism, besides selecting ionic species, has been so designed as to preserve the quality of the final selected image (*6*). In the instrument shown in Fig. 2, the ions are first deflected through 90°, then selected by a slit as a function of their momentum, and reflected by an electrostatic mirror in which the ions of high energy are eliminated. The selected ions are then deflected again through 90° in the second part of prism, and finally are detected. The mass resolving power of magnetic prism is of the order of 300, which allows a precision of selection of every mass unit of 1-300.

Detection-Display System

The selected ion-distribution image is then converted into an electron image by an image converter, and these electrons produce an image on a fluorescent screen or a photographic plate. The necessity of using an ion-to-electron image converter is because of the very weak response of most fluorescent screens or photographic plates to ions.

Finally, by changing the setting of the mass spectrometer, one can observe successively on the screen, or record on a photographic film, the images of distribution of different varieties of ions emitted from the surface of the specimen. Some accessories for this instrument are of interest to biologists. One is an electrostatic analyzer that improves the mass resolution, and with it the mass spectrum of a selected area of the specimen (from 10 to 50 μm in diameter) can be obtained with a resolution of the order of 5000. This may be very useful, as we shall see later, in distinguishing between monoatomic and polyatomic ions having the same mass unit. Another is a microchannel plate that allows the direct detection of the ion image without the help of the ion-to-electron image converter (*7*).

FUNCTIONING OF THE ION MICROSCOPE

With a primary-ion beam density of 0.1 $\mu A/cm^2$ (6×10^5 ions/μm^2/sec), the erosion rate of the specimen is typically of the order of 1-10 atomic layers/sec. Under these conditions, a biological section 1 μm thick is generally completely eroded in 300-3000 sec. As we shall see, this erosion time depends on the chemical and physical state of the matrix of the specimen. During that time, two working modes can be used: qualitative analysis by mass spectrometry, or the imaging mode.

Qualitative Analysis

The primary beam, with a diameter depending on the area of interest, is focused on the surface of the specimen,

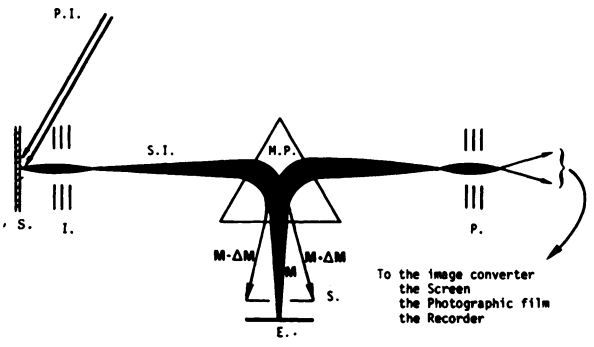

FIG. 2. Schematic diagram of analytical ion microscope. PI = primary ions, S = specimen, I = immersion electrostatic lens, SI = secondary ions, MP = magnetic prism, M = selected mass, E = electrostatic mirror, S_1 = selection diaphragm, P = projection lens.

and the mass spectrum of the sputtered secondary ions is recorded. A complete spectrum in the m/e range from 1 to 300 is obtained in a time of the order of 1 min, corresponding to the erosion of about 60 atomic layers. In any biological material, a considerable number of peaks are observed because a given atom A may be emitted either as monoatomic ion A^+ or as multicharged ions A^{++}, A^{+++}, or cluster ions such as A_n^+, AB^+, ABC^+, etc. In an organic matrix, many of these cluster ions are formed of $C_nH_m^+$, with n and m = 1, 2, 3 . . . . As a result of the emission of cluster ions, considerable interference may be observed with a low mass resolution of 300. The mass resolving power is defined as $M/\Delta M$, where M is the mass of the ion and ΔM the smallest difference of mass that can be distinguished. With a resolution of 300 it is only possible to resolve one mass unit, and one cannot distinguish a mass defect between a given monoatomic ion and a cluster ion of the same mass unit (e.g., $^{56}Fe^+$ and $^{40}Ca^{16}O$ have the same mass unit, 56).

A mass resolution of 5000, which is now obtained on most modern instruments, is generally sufficient to resolve most mass interferences.

Imaging Mode

The secondary-ion beam, selected by the magnetic prism and carrying the image of only one variety of ion, enters the image converter, where the ions are converted into electrons. These electrons can then strike a fluorescent screen, where the image is directly observed. With an optical telescopic lens system, the magnification is 1000× for a field of view of 250 μm. The electron image can also be recorded on a photographic film at a magnification of 110×. The exposure time varies from a fraction of a second to several hundred seconds, depending on the concentration of the imaged element and its useful yield, as discussed below.

CHARACTERISTICS OF THE ION MICROSCOPE

Resolution

The resolution of this instrument at the surface of the image is 1 μm (0.5 μm at the center of the image) for an imaged surface area 250 μm in diameter. The resolution in depth varies from 1 to 1000 nm depending on the volume to be sputtered to obtain the image: for a given element, the number of atomic layers that must be sputtered to obtain enough ions may vary from 1 to 3000 depending on the concentration. These images can be considered tomograms since they represent the distribution of a given nuclide with a resolution of 1 μm in a section whose thickness varies from 1 to 1000 nm.

With an image area 250 μm in diameter and with a lateral resolution of 1 μm, there are $125^2 \times \pi \simeq 50{,}000$ spatial information pixels, and this information is recorded on a photographic film. In normal conditions of primary-ion bombardment, the sputtering rate of the specimen is typically 1 to 10 atomic layers per second; thus a time exposure of 1 sec records on the film the distribution of a given nuclide in an extremely thin layer (0.3–1 nm).

Sensitivity

Factors influencing sensitivity. This varies greatly with many factors, briefly discussed here. For more information, the reader is referred to earlier detailed reviews (*8–12*). The two main factors are the ionization ratio of the imaged element and the collection efficiency of the instrument.

Ionization ratio. In the sputtering process, atoms are emitted either neutral or ionized. Since any atom emitted uncharged is lost for analysis, the sensitivity will depend in good part on the ionization ratio, defined for example as $\tau = N(A^+)/N(A)$ for positive ions, where $N(A^+)$ is the number of A atoms emitted as positive ions and N(A) the total number of A atoms, charged or uncharged, emitted during the same time. τ varies greatly from one element to another depending on both the ionization potential and the electron affinity of the element. For example, for positive secondary ions emitted under oxygen bombardment, τ is very high for Na^+ (0.8) and similarly for any element of low ionization potential (Groups 1, 2A, and 3A of the Periodic Table), although it is very low for gold, where $\tau\ (Au^+) = 10^{-6}$. For negative secondary ions, τ is high for elements of high electron affinity (Groups 6A and 7A).

Other factors such as the chemical bonds of the elements in the specimen (*6*) or the nature of the primary ions (*11*) may also greatly influence the ionization ratio. As an example, electronegative elements such as oxygen, when used for primary ions, enhance the ionization ratio of positive secondary ions, although elements of low electronegativity, such as cesium, enhance the ionization ratio of negative secondary ions.

Collection efficiency of the instrument. The collection efficiency or transmission of the instrument, η, is defined for positive ions as $\eta = n(A^+)/N(A^+)$, where $N(A^+)$ is the number of ionized atoms A^+ emitted from a given area of the sample, and $n(A^+)$ is the number of ions arriving at the detector from the same area during the same time. η is dependent upon the instrument, and for the instrument used in this study it is of the order of 5%.

Finally, the sensitivity is evaluated by the useful yield, defined as $\tau_u = \tau\eta$.

Maximum theoretical sensitivity. The term sensitivity is defined here assuming a perfect detector and no background signal. In ion microscopy, this optimal sensitivity is not very different from the practical detectability, since the quantum yield of the detector is close to 1 and the background is very low. Let us consider

optimal conditions, with an element with τ close to 100%, a transmission η of the instrument of 5%, and a resolution of 1 μm at the image. Since the impact of a single ion on a detector such as a microchannel plate is sufficient to produce a light signal, an average of 20 ions must be emitted from 1 μm^2 of the sample to be registered on a photographic film as a point of light and localized with a precision of 1 μm. This number varies greatly in practice due to statistical fluctuations.

Practical sensitivity. The total number N of atoms that must be sputtered from the specimen to obtain n_i^+ ions of atom i of $\tau_u = \tau_u$ (i) at the detector is given by $N = n_i^+/[\tau_u(i)C_i]$, where C_i is the atomic concentration of atom i.

Secondary ions emitted from the surface of the specimen can be registered in a electronic counting system or on a photographic film. When an image converter is used, one collected ion produces an average of four or five electrons, and each electron may activate several silver halide crystals in the film. The quantum yield Q of the converter is of the order of 0.8. Calibration of the photographic film being used has shown that for a 110× magnification 3000 ions emitted from 1 μm^2 of the specimen must be collected in the image converter to obtain an optical density on the film equal to 0.7 (*7*); this corresponds to an impact of about one electron/μm^2 on the film.

For a very emissive element such as Na^+, with $\tau_u = 5 \times 10^{-2}$, in an atomic concentration of 10^{-2}, the optical density of 0.7 on the film is obtained when the number of sputtered atoms is $N = 3 \times 10^3/(5 \times 10^{-2} \times 10^{-2}) = 6 \times 10^6$ atoms. This corresponds to about one atomic layer per square micron. If the sputtering rate is of the order of 1 atomic layer/sec, the exposure time will be 1 sec. As an example, the Na^+ image of Fig. 3 was obtained in 1 sec.

For the same element at a concentration of 3×10^{-6} (3 ppM), the same number of collected ions will be obtained at the cost of sputtering about 3×10^3 atomic layers, or a thickness of about 1 μm.

For some other element at the same concentration of 10^{-2} but with a τ_u of 10^{-4}, the optimal density on the film will be obtained at the cost of sputtering 300 atomic layers.

Precision in a Local Quantitative Analysis

Since the number of ions emitted from a given area of the specimen depends on the local concentration C_i of a given element i, and since the resolution at the image is 1 μm, it is possible by ion microscopy to measure the local concentration of a given element in a very small volume of tissue. Theoretically, the atomic concentration of element i is given by $C_i = n_i/(\rho \, v \, \tau_u)$, where n_i is the number of collected ions under a given surface, ρ the atomic density, and v the volume of the specimen sputtered under the same surface. The number of collected ions can be counted by an electronic counting system, or derived from the photographic film by microdensitometry. However, the methods of quantitative analysis are generally complicated because it is also necessary to know the exact value of the useful yield τ_u of the element and, as we have seen, τ_u may vary widely with many factors such as the nature of the element to be analyzed, its chemical state in the specimen, and the nature of the primary ions. Thus a standard must be used in a chemical form as similar as possible to that of the specimen. Different approaches have been proposed (*13–17*).

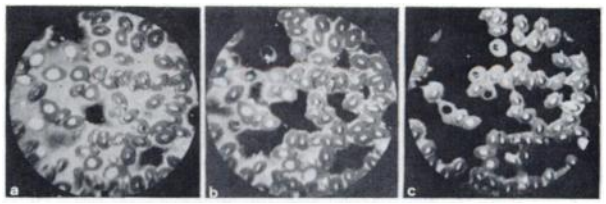

FIG. 3. Sodium image ($^{23}Na^+$) of surface of smear of nucleated red blood cells deposited on a gold specimen holder: a = 30th sec after beginning of primary-ion bombardment, b = 1st min, c = 2nd min. Imaged area = 250 μm diam. Exposure time = 1 sec for each figure. In Fig. 3a areas corresponding to plasma, cytoplasm, and nuclei can easily be distinguished. After 2 min of ion bombardment, (Fig. 3c), plasma layer and some nuclei have been completely etched.

Precision in a given measurement. If we want to obtain a given precision of p% in a measurement, it is necessary to collect at least n_i^+ ions equal to $10^4/p^2$. Let N be the total number of atoms of the specimen that must be sputtered to obtain n_i^+ ions, τ_u the useful yield of ions i, and C_i the atomic concentration of ion i. Then $n_i^+ = N \tau_u C_i$.

The sputtering of N target atoms will then give a precision p as derived from $p^2 = 10^4/(N\tau_u C_i)$. Assuming there are 10^7 atoms in 1 μm^2 of the surface of the specimen, and that $C_i = 10^{-2}$ and $\tau_u = 10^{-3}$, we obtain $p^2 = 10^4/(10^7 \times 10^{-2} \times 10^{-3}) = 100$, or a precision p = 10% for the sputtering of only one atomic layer.

A better precision of p = 3% will be obtained for the same element i at the same concentration, at the cost of sputtering a larger number of atoms such as $N = 10^4/(9 \times 10^{-2} \times 10^{-3}) \simeq 10^8$ atoms, which corresponds to the sputtering of 10 atomic layers.

Then for a section 1 μm thick, corresponding to about 3000 atomic layers, and with an element having $\tau_u = 10^{-3}$, the lowest concentration that can be studied with a precision of 3% is $C_i = 10^4/30 \times 10^9 \times 10^{-3} \times 9 \simeq 3 \times 10^{-5} \simeq 30$ ppM.

Take as an example sodium in a dried biological tissue at a concentration of 1%. If τ_u (Na^+) = 5×10^{-2}, a precision of 3% in the measurement will be obtained when the number of sputtered atoms is $N = 10^4/(9 \times 5 \times 10^{-2} \times 10^{-2}) \simeq 2 \times 10^6$ atoms, which corresponds to the sputtering of less than one atomic layer.

APPLICATIONS

Preparation of a Biological Specimen

A perfectly flat and equipotential surface of the specimen must be used for these studies. Preparation will be different depending on the tissue to be studied.

In the applications presented here, the tissues were prepared according to the conventional methods used in electron microscopy: fixation in glutaraldehyde, post-fixation in osmium tetroxide, and dehydration in alcohol. The tissue is then embedded in Epon, sectioned at 2 μm with an ultramicrotome, and deposited on a pure gold specimen holder.

Examples of Applications

Figure 3 shows the distribution of sodium ($^{23}Na^+$) at the surface of a smear of nucleated red blood cells from a frog. The same area is imaged in a, b, and c at different times after the beginning of the primary ion bombardment. The plasma, the cell cytoplasm, and nuclei are easily recognized. In 3a, obtained after the first few seconds of primary ion bombardment, the plasma and cell nuclei appear as bright areas with the cytoplasm darker. As ion bombardment continues, the plasma areas become dimmer and disappear completely after about 2 min (Fig. 3c), leaving only the cells. The cell cytoplasm and nucleus are etched at different rates; the nucleus disappears before the cytoplasm, and the image persists for approximately 15 min under normal conditions. The fact that the rate of etching varies for the different cellular and extracellular components must be taken into consideration in any attempt at local quantitative analysis of such a specimen. For example, the greater brightness of the plasma in the analysis of $^{23}Na^+$ is the result of both a higher concentration of sodium and a more rapid etching of the plasma regions by the primary beam.

Indium images. Twenty-four hours after intravenous injection of 0.5 mg of stable indium as a soluble salt (indium sulfate), the kidneys and the cardiac tissue of a rat were removed and prepared as previously described. The distribution of stable $^{23}Na^+$ and $^{115}In^+$ emission from the same area of the surface of a kidney section are shown on Figs. 4a and 4b. Although at a low concentration in this Epon section, $^{23}Na^+$ emission is very intense and the sputtering of only five atomic layers is sufficient to obtain the $^{23}Na^+$ image. A glomerulus (G) and several tubules are identifiable in this image. In Fig. 4b, $^{115}In^+$ is concentrated at many points corresponding to tubular areas. Electron microscopy study of a serial section corresponding to this specimen showed the presence of many lysosomes in the cells of the proximal tubules.

We have demonstrated previously (*18*) that the bright points of indium visualized with the ion microscope correspond to lysosomes seen with the electron microscope; thus it was possible to describe the cellular mechanism of concentration and elimination of indium by the kidney.

Figure 5 shows the distribution of $^{115}In^+$ on the surface of the section of cardiac tissue. Again, indium is concentrated in very small areas and the combined electron microscopic study has shown that these areas correspond to special lysosomes in the cardiac muscle cells.

Gallium images. The kidney, liver, bones, and bone marrow of a rat were removed 24 hr after intravenous

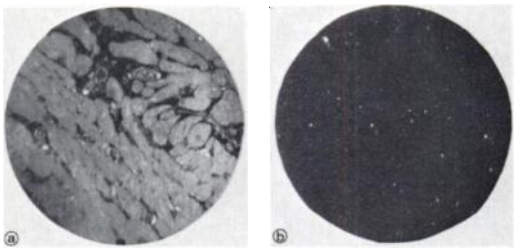

FIG. 5. $^{23}Na^+$ image (a) and $^{115}In^+$ image (b) obtained from same area (250 μm diam.) of cardiac section. Histological structures can be observed on sodium image (a). Indium image appears as very small light points (b), showing that this element is focally concentrated in cardiac muscle cells.

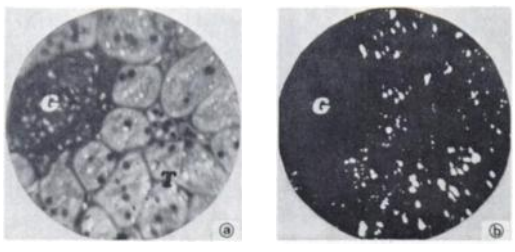

FIG. 4. $^{23}Na^+$ image (a) and $^{115}In^+$ image (b) obtained from same area of section of kidney. Imaged area = 250 μm diam. On sodium image—obtained in 5 sec, corresponding to pulverization of about five atomic layers—areas corresponding to glomerulus (G) and several tubules are obvious. Indium image, obtained in 500 sec, shows that this element is focally concentrated in many parts of tubular area.

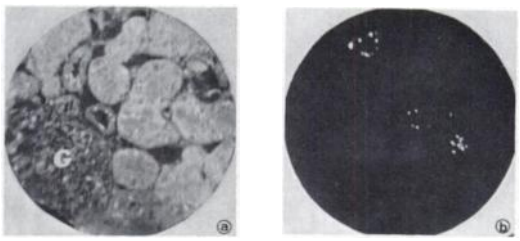

FIG. 6. $^{23}Na^+$ image (a) and $^{69}Ga^+$ image (b) obtained from same area (250 μm diam.) of a kidney section. Histological structures can be recognized in sodium image (a), where glomerulus (G) and several tubules are observed. On gallium image (b), this element appears as light points corresponding to local concentration in only three tubules.

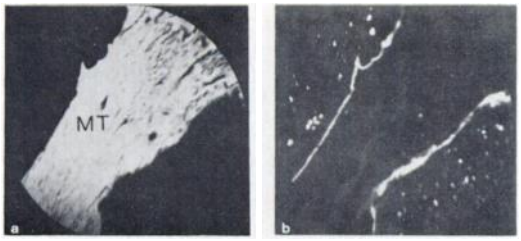

FIG. 7. $^{40}Ca^{+}$ (a) and $^{27}Al^{+}$ (b) images obtained from surface of bone section. Specimen is bone biopsy from patient with dialysis osteomalacia. Aluminum is localized at surface of calcified tissue, where it appears as bright lines; in soft tissue it appears as bright points corresponding to macrophages.

injection of 1 mg of stable gallium as a soluble salt (gallium citrate). Figures 6a and 6b show the distribution of $^{23}Na^{+}$ and $^{69}Ga^{+}$ on the surface of a kidney section, with the same area imaged in the two figures. Gallium is concentrated in only three tubules, each bright point corresponding to a local concentration of gallium. A similar combined study by electron microscopy has shown that these points correspond to intracellular lysosomes.

A similar study has been made on sections from liver, trabecular bone, and bone marrow. Gallium is concentrated in the lysosomes of hepatocytes and in small vacuoles of bone-marrow reticulocytes. In bone, gallium is concentrated at the surface of the calcified matrix. A detailed description of these results will be given in a future report.

Calcium and aluminum images in a hard tissue. Figures 7a and 7b show the distribution of $^{40}Ca^{+}$ and $^{27}Al^{+}$ on the surface of a bone section, a biopsy from a patient with dialysis osteomalacia. Aluminum is mainly localized at the surface of the calcified tissue (Fig. 7b).

FOOTNOTE

* The instrument used for this study was a CAMECA IMS 300.

ACKNOWLEDGMENT

Sources of support for this work were CNRS and INSERM.

REFERENCES

1. CASTAING R, SLODZIAN G: Microanalyse par émission ionique secondaire. In *Proceedings of the European Regional Conference on Electron Microscopy*, Delft, 1960, pp 169-172
2. CASTAING R, SLODZIAN G: Microanalyse par émission ionique secondaire. *J Microsc* 1:395-410, 1960
3. GALLE P: Sur une nouvelle méthode d'analyse cellulaire utilisant le phénomène d'émission ionique secondaire. *Ann Phys Biol Med* 42:84-94, 1970
4. GALLE P: Cellular microanalysis: a comparison between electron microprobe and secondary ion emission microanalysis. In *Microprobe Analysis as Applied to Cells and Tissues.* London/New York, Academic Press; 1974, pp 89-105
5. GALLE P: Microanalysis in biology and medicine, a review of results obtained with three microanalytical methods. *Scan Electron Microsc* 11:703-710, 1979
6. SLODZIAN G: Etude d'une méthode d'analyse locale chimique et isotopique utilisant l'émission ionique secondaire. Thesis Sci. Paris, Masson Ed., 1963
7. CHAINTREAU M, SLODZIAN G: Observation des images données par l'analyseur ionique au moyen d'une galette de microcanaux. *J Microsc Spectrosc Electron* 3:457-462, 1978
8. ANDERSEN CA: Analytic methods and applications of the ion microprobe mass analyser. In *Microprobe Analysis.* NewYork, John Wiley and Sons, 1973, pp 531-553
9. BERNHEIM M, SLODZIAN G: Emission d'ions négatifs en présence de cesium. *J Microsc Spectrosc Electron* 2:291-292, 1977
10. BLAISE G: Fundamental aspects of ion microanalysis. In *Material Characterization using Ion Beams.* New York, Plenum Publishing Corporation, 1978, pp 143-238
11. KROHN VE: Emission of negative ions from metal surfaces bombarded by positive cesium ions. *J Appl Phys* 33:3523-3528, 1962
12. SLODZIAN G: Some problems encountered in secondary ion emission applied to elementary analysis. *Surf Sci* 48:161-186, 1975
13. ANDERSEN CA, HINTHORNE JR: Thermodynamic approach to the quantitative interpretation of sputtered ion mass spectra. *Analyt Chem* 45:1421-1438, 1973
14. BURNS-BELLHORN MS, FILE DM: Secondary ion mass spectrometry (SIMS) of standards for analysis of soft biological tissue. *Analyt Biochem* 92:213-221, 1979
15. LODDING A, GOURGOUT JM, PETERSSON LG, et al: Aspects of quantitative determination by ion probe of fluorine concentrations in apatites. *Z Naturforsch* 29a:897-900, 1974
16. MORGAN AE: Further developments in semiquantitative SIMS. *J Microsc Spectrosc Electron* 5:221-229, 1980
17. SLODZIAN G, HAVETTE A: Quelques résultats d'analyse quantitative sur des silicates. *J Microsc Spectrosc Electron* 2:81-83, 1977
18. GALLE P: Physiologie Animale—Mécanisme d'élimination rénale de deux éléments du groupe IIIA de la classification périodique: l'aluminium et l'indium. *C R Acad Sci (Paris)* 292:91-96, 1981